Adsorption (2014) 20:623–630
DOI 10.1007/s10450-014-9607-y

Adsorption of carbonyl sulfide on modified activated carbon under low-oxygen content conditions

Xueqian Wang · Yixing Ma · Ping Ning · Juan Qiu · Xiaoguang Ren · Ziyan Li · Wei Chen · Wei Liu

Received: 25 September 2013 / Revised: 30 January 2014 / Accepted: 31 January 2014 / Published online: 20 February 2014

Abstract Activated carbon sorbents impregnated with KOH, $Fe(NO_3)_3$, $Cu(NO_3)_2$, $Zn(NO_3)_2$ or $Co(NO_3)_2$ and their applications in catalytic oxidation reaction of COS were investigated. The results showed that the activated carbon modified with 10 % (mass percentage) KOH enhanced the adsorption ability significantly. And it was also found that the oxygen content and temperature were the two most important factors in the COS adsorption. Further investigation on the pore structures of the samples with X-ray photoelectron spectroscopy indicated that an adsorption/oxidation process happened in the KOH modified activated carbon in which the major existing forms of sulfur were SO_4^{2-} and S species. The oxidation of COS suggested that KOH in the micropores may play a catalytic role during the adsorption. On the other hand, we found that the desorption activation energy from KOHW was higher than that from AC by the CO_2-TPD spectra, which indicated the adsorption of CO_2 on KOH impregnated activated carbon was stronger. The strong adsorption could be attributed to the basic groups on the activated carbon surface. In conclusion, the activated carbon impregnated with KOH promises a good candidate for COS adsorbent.

Keywords Carbonyl sulfide · Modified activated carbon · Adsorption

X. Wang · Y. Ma · P. Ning (✉) · J. Qiu · X. Ren · Z. Li · W. Chen · W. Liu
Faculty of Environmental Science and Engineering, Kunming University of Science and Technology, 650500 Kunming, China
e-mail: wxqian3000@aliyun.com

1 Introduction

Recently, there has been renewed interest in carbonyl sulfide which is generated when sulfur is removed from chemical feedstocks (Rhodes et al. 2000). COS, which exists in natural gas, liquefied petroleum gas, water gas and coal gas (Wang et al. 2011; Williams et al. 1999), is one of the major existing forms of organic sulfur compounds as well as an odor-causing compound which is listed in the US Clean Air Act as a hazardous air pollutant (Sattler et al. 2009). Over the last two decades, it has become increasingly apparent that recent emission of sulfur compounds into the atmosphere is unacceptably high (Rhodes et al. 2000).

COS is also commonly released into the atmosphere and it is found in trace amount in the troposphere (1.339×10^{-3} mg/m^3) where its lifetime has been estimated at 2–7 years (Rhodes et al. 2000; Liu et al. 2008). Although the chemical reactivity of COS in the atmosphere is low, it contributes to the formation of SO_2 and to the promotion of photochemical reactions (Wang et al. 2008). The high sulfur content in industrial feedstocks not only pollutes the environment by causing acid rain, but also brings economic problems to the petrochemical industry (Williams et al. 1999; Zhang Y et al. 2004; Zhao et al. 2010; Huang et al. 2005). On the other hand, sulfur is also defined as a non-specific catalyst poison that can dramatically reduce the catalytic activities (Jackson et al. 1996). Level of sulfur as low as 2.5 mg/m^3 can effectively poison the modern bi-metallic reforming catalysts, and as little as 4 mg of sulfur on the surface of 1 g Fe–Cu–K catalyst that used in the Fischer–Tropsch process can decrease the observed activity by about 50 % (Rhodes et al. 2000; Wang et al. 2008). Apart from affecting the catalysts, the presence of sulfur in feedstocks can also bring increased

corrosion of the reactors that used in refining processes (Rhodes et al. 2000). Raw materials that have undergone desulfurization, consequently, are less hazardous and less corrosive, and more appropriate for manufacturing odor-free products (Rhodes et al. 2000; Williams et al. 1999).

COS is one of the major existing forms of organic sulfur compounds. COS, due to less acidic and less polar than H_2S, is harder to be removed with conventional adsorbents (Svoronos and Bruno 2002; Sparks et al. 2008; Huang et al. 2006a). To date, direct removal of sulfur contaminants via adsorption is still a particularly attractive method for achieving low sulfur levels (Toops and Crocker 2008). Different types of adsorbents, including supported metal oxides (where the support is typically alumina or carbon) (Jackson et al. 1996; Sparks et al. 2008; Sakanishi et al. 2005; Thomas et al. 2003; West et al. 2001), mixed metal oxides, metal ion-exchange zeolites and activated carbons, have been investigated extensively in recent years. Carbon-based adsorbent such as activated carbon has been widely applied in the purification procedures of gas (Sparks et al. 2008; Sakanishi et al. 2005; Ning et al. 2010), whereas coal-based carbon is an attractive alternative for its low cost. The adsorption capacity of the activated carbon is generally enhanced by modification such as impregnation with transition metals (Rhodes et al. 2000). Kinya et al. reported that impregnation of Fe on activated carbon greatly enhanced its adsorption ability for both COS and H_2S at 300–450 °C. The adsorption capacities of COS over AC–PA (a commercial active carbon powder), AC–PO (a commercial active carbon particle), RP–PO (red pine derived active carbon particles), YLFe–PO (brown coal-derived activated carbon particles modified with Fe), and YL–PO (brown coal-derived activated carbon particle) were 0.000, 0.039, 0.234, 2.860, and 2.600 mg COS/g activated carbon at 400 °C, respectively (Ning et al. 2010). Sattler et al. found that VPR, BPL and Centaur were able to adsorb COS efficiently, and the COS adsorption capacities for the three types of activated carbon were 1.8, 2.1 and 3.5 mg COS/g activated carbon at 70–80 F and 17 % RH, respectively (Sattler and Rosenberk 2006).

In this work, the activated carbon-based adsorbents for COS were prepared with impregnation of various types of modifiers, and their adsorption effects on COS were tested. The performances of these modified activated carbons were evaluated by the breakthrough data of COS. The experimental conditions, such as the type of impregnate, reacting temperature and oxygen content, were studied to achieve the optimum conditions for adsorption of COS. We also examined the changes in micro-mechanism of produced adsorbent surface by measuring specific surface area and inspecting pore structure. Nitrogen adsorption at 77 K was employed to characterize the pore structure of the adsorbents such as pore size distribution and surface area. The external surfaces of the adsorbents were also studied using X-ray photoelectron spectroscopy (XPS). CO_2-TPD technique was used to estimate binding energy and desorption activation energy which were used to evaluate the adsorbents.

2 Materials and methods

2.1 Experimental materials

Transition metals (such as Cu, Fe) have been studied for the adsorption and oxidation processes. According to the study by Ning et al. using $Cu(CH_3COO)_2$ on modified activated carbon on adsorption of H_2S, CS_2, COS, and PH_3, Cu improved the adsorption and oxidation (Ning et al. 2011; Wang et al. 2012). In our primary investigation, activated carbon impregnated with $Cu(NO_3)_2$–CoPcS–KOH promises a good candidate for COS adsorbent. Thus Cu, Zn, Fe, Co were chosen in this work. Coal-based activated carbon was used as supports in this study (Chang Ge Qian Yuan Chemical Factory, Henan, China). The supports (10 g ± 0.1 g) were washed three times by 150 mL of distilled water at 70 °C to remove soluble impurities, and then were dried for 12 h at 110 °C. Afterwards, the activated carbon was impregnated with 10 % KOH, 0.1 mol/L $Cu(NO_3)_2$, 0.1 mol/L $Zn(NO_3)_2$, 0.1 mol/L $Co(NO_3)_2$ or 0.1 mol/L $Fe(NO_3)_3$ at ambient temperature, respectively. For the impregnation, to approximately 50 mL of impregnating solution was added 10 g of AC, and the suspension was stirred for 24 h, after that, the suspension was filtrated and the adsorbent was dried for 12 h at 130 °C. The samples were marked as KOHW (KOH-impregnated activated carbon), CuW ($Cu(NO_3)_2$-impregnated activated carbon), ZnW ($Zn(NO_3)_2$-impregnated activated carbon), CoW ($Co(NO_3)_2$-impregnated activated carbon), and FeW ($Fe(NO_3)_3$-impregnated activated carbon), respectively.

2.2 COS adsorption experiments

The COS adsorption experiments were carried out in a chamber in which pressure was controlled to be slightly below atmospheric pressure for avoiding escape of COS gas from the adsorption column. The measurements were performed with model gases at a space velocity of 1,200 h^{-1} at standard temperature and pressure which were regulated by a mass flow meter. The model gas flow was composed of nitrogen and 3,020 mg/m^3 COS which were mixed in a mixer (CY-1298, made by Suzhou Richtreatment Environment Technologies, Inc) evenly with micro-oxygen and subsequently introduced into the adsorption bed unit. This adsorption reaction was conducted in a quartz columnar reactor with 9 mm inner diameter and 60 mm in length. A total of 3.5 g of adsorbents was packed into the reactor for

each test, and the experiment was stopped when the absorbent was saturated. COS was determined by off-gas chromatography. The "breakthrough time" is defined as the time at which the COS outlet concentration reaches 10 % of the inlet concentration according to breakthrough curves. After the experiment ended, the adsorption capacity of COS, depending on the quality of the sorbent, was calculated with the corresponding integral according to formula (1) under various conditions of the breakthrough curves (Wang et al. 2009; Huang et al. 2006b; Xiao et al. 2008).

$$X = QC_0 \int_0^{t_s} \left(1 - \frac{C}{C_0}\right) dt/m \quad (1)$$

Where X is the adsorption capacity of COS, mg/g, Q, gas flow, m^3/min, t, the adsorption time, min, t_s, the breakthrough time (as $C/C_0 = 0.1$), C_0, the adsorption column entrance mass concentration, mg/m^3, C, the adsorption column outlet mass concentration, mg/m^3, m, adsorbent quality, g.

2.3 Determination of COS

COS was determined by gas chromatography-flame photometry under the following parameters: the flow rate of N_2 at 40 mL/min, column temperature at 50 °C, detector temperature at 96 °C, detection limit of 0.003 mg/m^3. The model of gas chromatography was GC-14C manufactured by Shimadzu (with flame photometric detector) with a polytetrafluoroethylene-packed column (GD–401 support).

2.4 Nitrogen adsorption isotherms

Multi-spot nitrogen adsorption meter NOVA2000e (Quantachrome Corp) was used to determine nitrogen adsorption isotherms under 77.350 K. Adsorption isotherms are used to accurately calculate specific surface area, volume of micropores, total volume of pores and micropore size distribution as well.

2.5 XPS measurements

Photoelectron spectra were obtained using XPS analyses, which were carried out using a Physical Electronics PHI 5600 spectrometer. The X-ray source was operated by an Al Kα anode with photo energy of *hv* 1,486.6 eV. The core level binding energy of C 1s for carbon at 284.8 eV was employed as an internal reference for calibration.

2.6 Temperature programmed desorption experiments (TPD)

TPD tests were carried out in a TPD device equipped with a thermal conductivity detector (TCD). The adsorbent material was introduced in a quartz tube and outgassed in nitrogen flow (50 cm^3/min) at 200 °C for 60 min. Afterwards, the adsorbent sample was cooled down to 20 °C, and then exposure to CO_2. Thereafter, the weakly retained adsorbate was removed by passing a N_2 flow at 20 °C for 2 h. The completion of the physidesorption process was determined by the zero baseline recovery in the TCD signal. Finally, the adsorbate still retained in the adsorbent was removed by heating the sample at a rate of 5–20 °C/min in the range of 20–500 °C within a constant N_2 flow, and maintaining the sample at 500 °C for one additional hour. The adsorbate evolved from the porous solid and present in the effluent stream was continuously monitored by means of the TCD.

The desorption activation energy E_d can be found out according to the following equation:

$$\ln\left(\frac{T_p^2}{\beta_H}\right) = \frac{E_d}{R}\left(\frac{1}{T_p}\right) + \ln\left(\frac{E_d}{Rk_0}\right) \quad (2)$$

Where R is the gas constant. T_p, the peak temperature of the TPD (K). β_H, heating rate (K/min). E_d, desorption activation energy (kJ/mol). k_0, the coefficient of desorption rate. If a series of TPD experiments are conducted at different heating rates, corresponding TPD curves and values T_p can be obtained, and thus a plot of $\ln(T_p^2/\beta_H)$ versus $1/T_p$ will yield a line with slope E_d/R. As a result, from the slope of the line, E_d can be found out.

3 Results and discussions

3.1 Effects of the types of modifiers

This work studied five types of adsorbents with different impregnates: KOHW, FeW, CuW, ZnW and CoW were measured and compared in a dynamic removal capacity for COS. The breakthrough curves of the five adsorbents are plotted in Fig. 1. Their breakthrough curves differ in their performance as COS adsorbents and clearly illustrate the efficiency of COS removal. Comparing with AC, FeW, CuW, ZnW and CoW, the KOHW sample showed a significant improvement in COS adsorption. The impregnation of KOH led to increases in breakthrough time as well as COS breakthrough capacities which were 0.6989, 0.7529, 1.490, 1.487, 2.964, 14.91 mg COS/g AC, FeW, ZnW, CoW, CuW, KOHW, respectively. The possible reason for high breakthrough capacities of KOHW was the basic groups on the activated carbon surface. The alkali hydroxides have effects not only on the pore size distribution but also on the reactivity of chemical groups on the activated carbon surface.

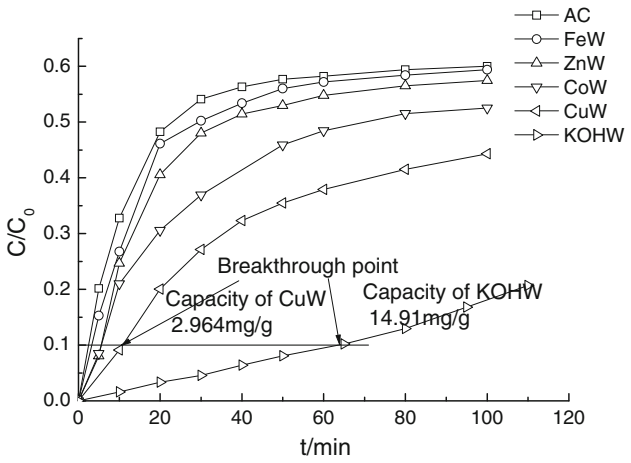

Fig. 1 Breakthrough curves of COS on different impregnants at 60 °C and 1.0 % O_2 (COS inlet concentration 3,020 mg/m^3)

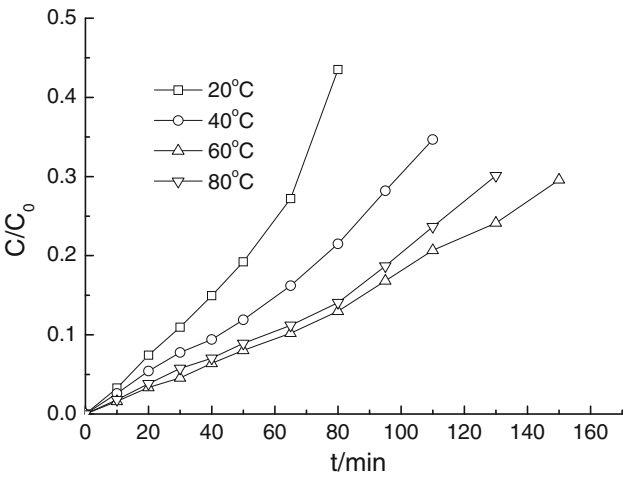

Fig. 2 COS breakthroughs in a KOHW fixed bed in the function of reaction temperature on (O_2 at 1.0 %, COS inlet concentration 3,020 mg/m^3)

3.2 Effects of operating conditions

3.2.1 Effects of reaction temperature

COS breakthroughs in the KOHW bed at 20, 40, 60 and 80 °C are presented in Fig. 2. Reaction temperature was found to be one of the most principal factors that affected the purification efficiency in the COS adsorption process with impregnated activated carbon. Figure 2 shows that the COS removal efficiency is enhanced significantly after increasing the reaction temperature. However, when the temperature reached a certain point (60 °C), the effect of reaction temperature on the COS adsorption efficiency no longer obviously increased with the increase of the temperature.

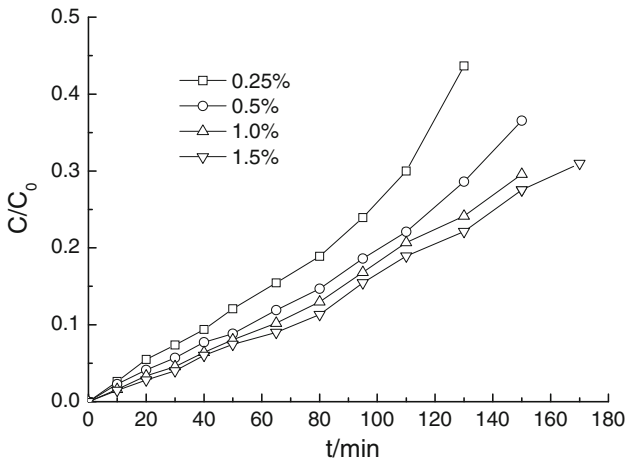

Fig. 3 COS breakthroughs in a KOHW fixed bed at 60 °C in the function of oxygen content (COS inlet concentration 3,020 mg/m^3)

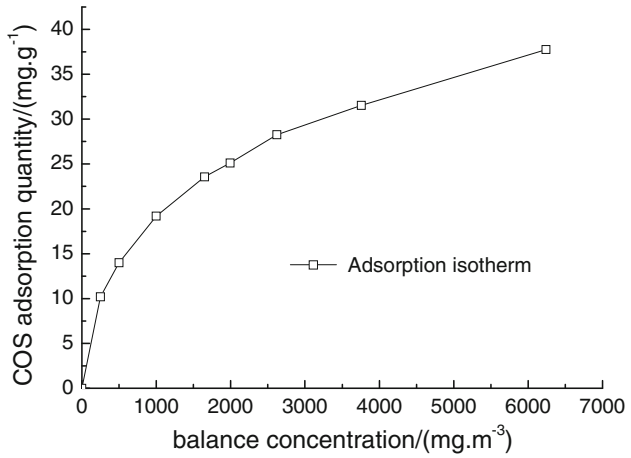

Fig. 4 Adsorption isotherm at 60 °C, O_2 1.0 %

3.2.2 Effects of the oxygen content

Figure 3 shows how the oxygen content affects the COS breakthroughs with KOHW at 60 °C at different oxygen contents of 0.25, 0.5, 1.0 and 1.5 %. The oxygen content is also one of the most important factors that influence the COS adsorption efficiency, and the efficiency increases significantly with the increase of oxygen content.

3.3 COS adsorption isotherm

The COS breakthrough curves on KOHW were drawn based on the points where the exit concentrations were 99 % of the entrance concentrations (C/Co = 99 %) of 250, 500, 1000, 1650, 2000, 2600, 3750, 6200 mg/m^3 at 60 °C, according to type (1) calculation of adsorption capacities (where the t_s should be the adsorption equilibrium time when C/Co = 99 %) based on which the adsorption isotherms of COS were determined. Figure 4

shows the adsorption isotherms of COS on KOHW of which high activity to COS was found, and the balance adsorption capacity increased significantly at 60 °C with 1.0 % of oxygen. Within the concentrations tested, COS adsorption isotherms on impregnated activated carbon were calculated according to Freundlich adsorption equation (Donohue and Aranovich 1998; Tian et al. 2009). The correlation stationary (R^2) was bigger than 0.99. Freundlich adsorption equation for adsorption of COS on KOHW at 60 °C was obtained after fitting as following:

$$q_e = 1.1063 c_e^{0.4089} \quad (3)$$

In the equation: q_e is balance adsorption capacity, g/g, c_e is balance concentration, mg/m^3.

3.4 Effects on pore size distribution

Figure 5 shows the change of pore size distribution of AC, KOHW and KOHWE which refers to the sample after COS adsorption. The BET surface area, average pore radius, micro- and total pore volume of three samples are listed in Table 1.

As seen from Fig. 5, most pores of the samples distribute below 2 nm. Their pore size distributions were analyzed by density function theory (DFT) (Oliver et al. 2005). Comparisons between AC and KOHW suggested that KOH modification resulted in a decrease in the volume of pores to smaller than 2 nm, and the most noticeable change happened in the micropore volume of pores with sizes ranging from 0.7 to 1.5 nm. These results illustrated that KOH was an effective component that loaded in the sorbent (László et al. 2001).

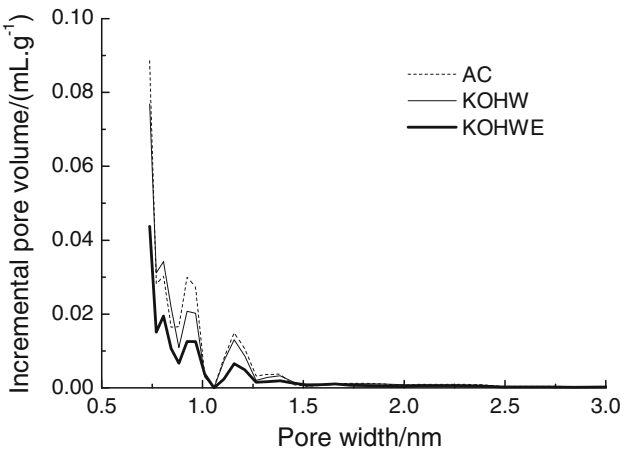

Fig. 5 Comparison of pore size distributions of KOH modified samples before and after COS adsorption

Table 1 Structural parameters calculated from adsorption of impregnated carbons

Samples	Specific surface area/ (m^2 g^{-1})	Total pore volume/ (ml g^{-1})	Micropore volume/ (ml g^{-1})	Average pore radius/nm
AC	827	0.446	0.385	1.07865
KOHW	704	0.378	0.329	1.07226
KOHWE	649	0.358	0.304	1.10455

Comparing the KOHW samples before and after adsorption, obvious differences only occurred in the micropore volume of pores with the size ranging from 0.7 to 1.5 nm. The range of variations in micropore size showed that activated COS was strongly adsorbed in the micropores.

The specific surface area S_{BET} of samples were calculated according to Brunauer–Emmett–Teller method from the linear part of the nitrogen adsorption isotherms, and V_{micro} were calculated using DFT method (Oliver et al. 2005). Structural parameters of impregnated activated carbon after modification and adsorption are shown in Table 1.

Comparing the outcomes from AC and KOHW samples, it was found that the impregnation resulted in a decrease in the volume of pores to smaller than 2 nm and the decrease accounted for 82.35 % in the total decrease of volume of pores. In addition, the surface areas decreased 14.87 % and the volume decreased 14.54 % in the KOH modified micropores. The pore distribution indicated that all micropores were influenced by the impregnation.

Figure 5 and Table 1 show the comparison between KOHW samples and KOHWE samples. KOHWE represents the exhausted adsorbent. Significant changes could be found in sorbent voidage during the process of COS adsorption. The surface areas decreased 7.81 % of which 7.60 % came from the decrease in micropore volumes after modification. Thus, it could be concluded that KOH in the micropores played a crucial role in COS oxidation and adsorption.

3.5 XPS analysis

To better understand the surface chemical change and the reaction mechanism during the adsorption, XPS was employed to deconvolve the high resolution C1s, O1s, K2p and S2p.

Table 2 shows the major surface element concentrations of KOHW samples before and after adsorption obtained by XPS analysis.

As shown in Table 2, the concentrations of C, O and K on the KOHW before adsorption were 79.39, 18.45 and 2.17 %, respectively. However, the concentrations of C, O, K and S on the KOHW after adsorption were 81.93, 15.06, 1.75 and 1.26 %, respectively. No S specie was found in freshly prepared KOHW adsorbent while it was observed in a big increase in the sample after adsorption (Ning et al. 2010; Huang et al. 2006a; László et al. 2001; Yi et al. 2011).

Figure 6 shows the XPS spectra of core level binding energy in S2p after adsorption/oxidation. The XPS fitting

Table 2 Elemental analysis of KOHW before and after adsorption using XPS

Sample	Before adsorption				After adsorption			
	C1s	O1 s	K2p	S2p	C1s	O1s	K2p	S2p
Area (cts-eV/s)	24835	13787	3353	0	73619	32668	7802	2536
Sensitivity factor	16.518	39.890	81.737	37.078	16.518	39.89	81.737	37.078
Concentration (%)	79.39	18.45	2.17	0	81.93	15.06	1.75	1.26

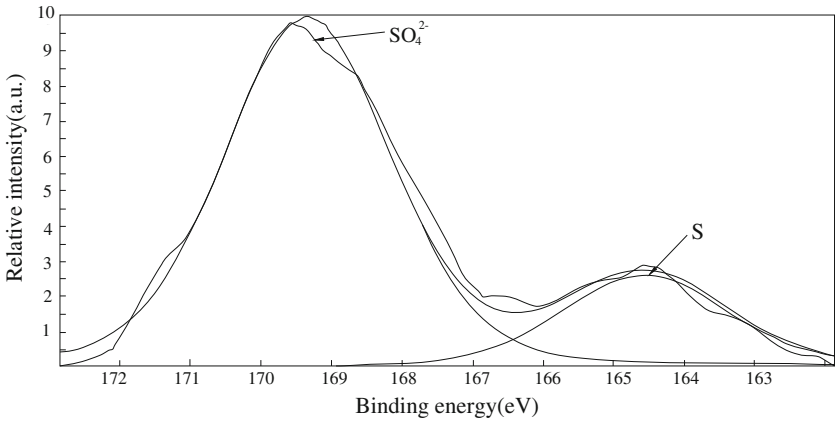

Fig. 6 The S2p peaks for the exhausted KOHW adsorbent

Table 3 XPS data of the S2p spectra and their possible S statuses after COS adsorption

S status	Before adsorption KOHW S2p	After adsorption KOHWE	
		SO_4^{2-}	S
Binding energy of S2p (eV)	–	169.35	164.57
fwhm (eV)	–	2.80	2.80
Calculated S percentage (%)	0	79.12	20.88

data of the S peaks, the possible S statuses, and their relative percentages are summarized in Table 3.

As shown in Fig. 6 and Table 3, the S2p peak that centered at 169.35 eV indicated the possible presence of SO_4^{2-}, and the peak that centered at 164.57 eV indicated the possible presence of S. It was also observed that the relative percentage of SO_4^{2-} (79.12 %) was more than that of S (20.22 %) in the sample after adsorption (Lee et al. 2003). The major existing forms of sulfur in the KOHWE samples were SO_4^{2-} and S species, demonstrating an oxidation process happened during the adsorption.

The results suggested that KOH may play a catalytic role in the oxidation of COS during the adsorption.

3.6 CO_2-TPD

TPD is a technique for surface analysis and it is usually used to estimate the binding energy between an adsorbate and an adsorbent as well as the activation energy of desorption, which are used to evaluate the adsorbent.

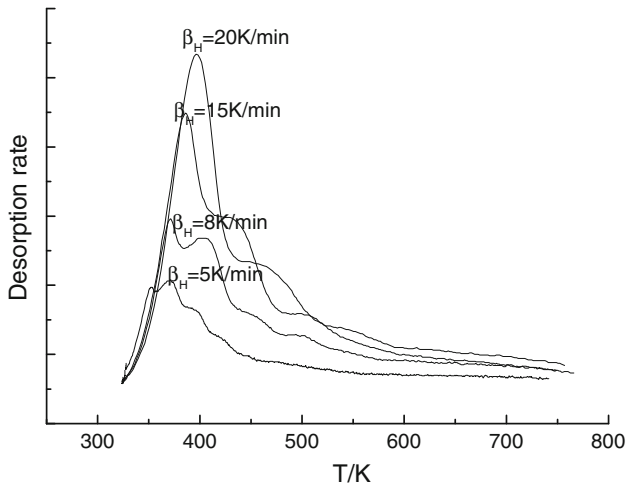

Fig. 7 Effect of β_H on the TPD spectrum for the desorption of CO_2 on AC (flow rate: 50 mL/min)

3.6.1 Spectrum analysis

Figures 7, 8 depict TPD spectra of AC and KOHW at the heating rate from 5 to 10 K/min, and it was found that there were two peaks in a TPD spectrum. This behavior could be assigned to adsorption sites with different strengths or to reactions of CO_2 with the active groups on the KOHW (Cui and Turn 2009; Yu et al. 2007; Li et al. 2008; Serrano et al. 2007).

3.6.2 Estimation of desorption activation energy

Once a series of the TPD spectra of CO_2 desorption on the activated carbon at different heating rates were available, the

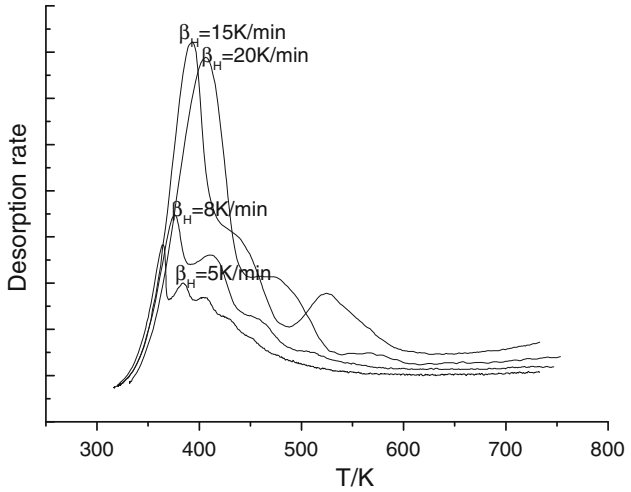

Fig. 8 Effect of β_H on the TPD spectrum for the desorption of CO_2 on KOHW (flow rate: 50 mL/min)

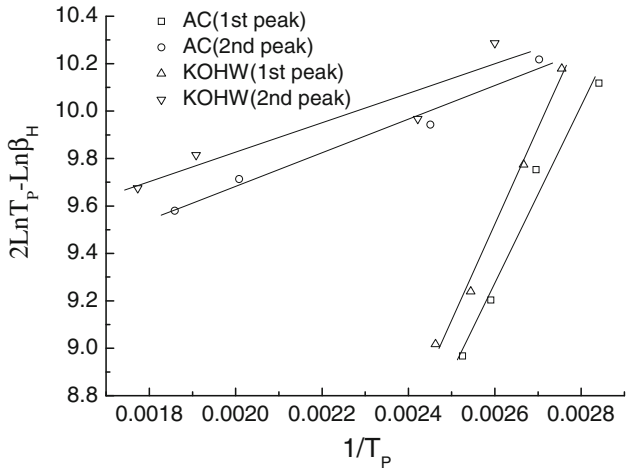

Fig. 9 Line dependence between $\ln(T_p^2/\beta_H)$ and $1/T_P$ for TPD of CO_2 on AC (flow rate: 50 mL/min)

desorption activation energy of CO_2 could be estimated using Eq. (2). The linear dependence on $1/T_p$ of $\ln(T_p^2/\beta_H)$ for the TPD of CO_2 on activated carbon is shown in Fig. 9, and the activation energy E_d can be found out from the slope of these lines. The desorption activation energy of CO_2 on these adsorbents are listed in Table 4 (Yu et al. 2007; Li et al. 2008).

If two peaks for the CO_2 desorption were found in a TPD spectrum, it possibly implied the desorption of CO_2 came from at least two kinds of adsorptive sites. Generally, the higher the desorption activation energy is, the more difficult the desorption is. In other words, the higher the desorption activation energy is, the stronger the adsorption is. The possible reason was the basic groups on the activated carbon surface which resulted in the higher desorption activation energy. Therefore, the basic groups contributed a significant increase in COS adsorption capacity.

Table 4 Activation energy for desorption of CO_2 on AC and KOHW

Active carbon	Peaks	T_p(K) corresponding to peak of TPD curves at different heating rate β_H (K/min)				Ed (KJ/mol)
		5	8	15	20	
AC	First peak	352	371	386	396	31.04
	Second peak	370	408	498	538	5.89
AC_{KOH}	First peak	363	375	393	406	33.43
	Second peak	383	413	524	564	8.422

4 Conclusions

The reactivity of modified activated carbon for COS adsorption was in a descending order as KOHW>CuW>CoW>ZnW>FeW. The oxygen content and temperature were two most important factors in the COS removal by KOHW. The adsorption ability of activated carbon impregnated with KOH was significantly enhanced and the sample showed a breakthrough capacity of 14.91 mg/g adsorbent at 60 °C with 1.0 % oxygen for removing COS. The micropores were influenced by all the impregnation, while the KOH favored the formation of surface functional groups. The decrease in the adsorbent's total pore volume after modification mainly occurred in the pores below 2 nm in diameter, especially in the range of 0.7–1.5 nm. The pore volume decreased significantly after modification and the decrease in micropore volume accounted for 82.4 % of the total volume change. After adsorption, the surface areas decreased 7.81 % of which 7.60 % came from micropore surface decrease.

The existing forms of sulfur on KOHW were proved to be SO_4^{2-} and S by XPS. No S species was found in freshly prepared KOHW, while SO_4^{2-} (79.12 %) and S (20.22 %) was observed in the sample after adsorption. It was likely that KOH in the micropores acted as a catalyst in the adsorption/oxidation process. On the other hand, it could be found from the CO_2-TPD spectra that the desorption activation energy from KOHW was higher than that from AC, indicating the adsorption of CO_2 on KOHW was stronger, which may due to the strong basic groups on the surface of activated carbon. In summary, KOH modified activated carbon can be employed as an efficient adsorbent for removing COS from a gas stream.

Acknowledgments This work was supported by the National Natural Science Foundation of China (No. 51268021, U1137603, 51368026), 863 National High-tech Development Plan Foundation

(No. 2012AA062504) and by Applied Basic Research Program of Yunnan (No. 2011FB027, 2011FA010).

References

Cui, H., Turn, S.Q.: Adsorption/desorption of dimethylsulfide on activated carbon modified with iron chloride. Appl. Catal. B **88**(1–2,29), 25–31 (2009)

Donohue, M.D., Aranovich, G.L.: Classification of Gibbs adsorption isotherms. Adv. Colloid Interface Sci. **76–77**(1), 137–152 (1998)

Huang, H.M., Young, N., Williams, B.P., Taylor, S.H., Hutchings, G.: COS hydrolysis using zinc-promoted alumina catalysts. Catal. Lett. **104**(1–2), 17–21 (2005)

Huang, H.M., Young, N., Williams, B.P., Taylor, S.H., Hutchings, G.: High temperature COS hydrolysis catalysed by γ-Al_2O_3. Catal. Lett. **110**(3), 243–246 (2006a)

Huang, C.C., Chen, C.H., Chu, S.M.: Effect of moisture on H_2S adsorption by copper impregnated activated carbon. J. Hazard. Mater. **136**(3), 866–873 (2006b)

Jackson, S.D., Leeming, P., Webb, G.: Supported metal catalysts: preparation, characterisation, and function IV. Study of hydrogen sulphide and carbonyl sulphide adsorption on platinum catalysts. J. Catal. **160**(2), 235–243 (1996)

Lee, Y.W., Kim, H.J., Park, J.W., Choi, B.U., Choi, D.K., Park, J.W.: Adsorption and reaction behavior for the simultaneous adsorption of NO–NO_2 and SO_2 on activated carbon impregnated with KOH. Carbon **41**(10), 1881–1888 (2003)

Li, J., Li, Z., Liu, B., Xia, Q.B., Xi, H.X.: Effect of relative humidity on adsorption of formaldehyde on modified activated carbons. Chin. J. Chem. Eng. 16(6), 871–875 (2008)

Liu, Y.C., He, H., Mu, Y.J.: Heterogeneous reactivity of carbonyl sulfide on α-Al_2O_3 and γ-Al_2O_3. Atmos. Environ. **42**(5), 960–969 (2008)

László, K., Tombácz, E., Josepovits, K.: Effect of activation on the surface chemistry of carbons from polymer precursors. Carbon **39**(8), 1217–1228 (2001)

Ning, P., Yu, L.L., Yi, H.H., Tang, X.L., Li, H., Wang, H.Y., Yang, L.N.: Effect of Fe/Cu/Ce loading on the coal-based activated carbons for hydrolysis of carbonyl sulfide.J. Rare Earths **28**(2), 205–210 (2010)

Ning, P., Wang, X.Y., Bart, H.J., Tian, S.L., Zhang, Y., Wang, X.Q.: Removal of phosphorus and sulfur from yellow phosphorus off-gas by metal-modified activated carbon. J. Clean. Prod. **19**(13), 1547–1552 (2011)

Oliver, T.M., Jugoslav, K., Aleksandar, P., Nikola, D.: Synthetic activated carbons for the removal of hydrogen cyanide from air. Chem. Eng. Process. **44**(11), 1181–1187 (2005)

Rhodes, C., Riddel, S.A., West J., Williams, B.P., Hutchings, G.J.: The low-temperature hydrolysis of carbonyl sulfide and carbon disulfide: a review. Catal. Today **59**(3–4), 443–464 (2000)

Sakanishi, K.,Wu, Z.H., Matsumura, A., Saito, I., Hanaoka, T., Minowa, T., Tada, M., Iwasaki. T.: Simultaneous removal of H_2S and COS using activated carbons and their supported catalysts. Catal. Today **104**(1), 94–100 (2005)

Sattler, M.L., Garrepalli, D.R., Nawal, C.S.: Carbonyl sulfide removal with compost and wood chip biofilters, and in the presence of hydrogen sulfide. J. Air Waste Manag. Assoc. **59**(12), 1458–1467 (2009)

Sattler, M.L., Rosenberk, R.S.: Removal of carbonyl sulfide using activated carbon adsorption. J. Air Waste Manag. Assoc. **56**(2), 219–224 (2006)

Serrano, D.P., Calleja, G., Botas, J.A., Gutierrez, F.J.: Characterization of adsorptive and hydrophobic properties of silicalite-1, ZSM-5, TS-1 and Beta zeolites by TPD techniques. Sep. Purif. Technol. **54**(1,15), 1–9 (2007)

Svoronos, P.D.N., Bruno, T.J.: Carbonyl sulfide: a review of its chemistry and properties. Ind. Eng. Chem. Res. **41**(22), 5321–5336 (2002)

Sparks, D.E., Morgan, T., Patterson, P.M., Tackett, S.A., Morris, E., Crocker, M.: New sulfur adsorbents derived from layered double hydroxides I: synthesis and COS adsorption. Appl. Catal. B **82**(3–4), 190–198 (2008)

Thomas, B., Williams, B.P., Young, N., Rhodes, C., Hutchings, G.J.: Ambient temperature hydrolysis of carbonyl sulfide using γ-alumina catalysts: effect of calcination temperature and alkali doping. Catal. Today **86**(4), 201–205 (2003)

Tian, S.L., Mo, H., Zhang, R.F., Ning. P., Zhou, T.H.: Enhanced removal of hydrogen sulfide from a gas stream by 3-aminopropyltriethoxysilane-surface-functionalized activated carbon. Adsorption **15**(5–6), 477–484 (2009)

Toops, T.J., Crocker, M.: New sulfur adsorbents derived from layered double hydroxides II. DRIFTS study of COS and H_2S adsorption. Appl. Catal. B **82**(3–4), 199–207 (2008)

Wang, H.Y., Yi, H.H., Ning, P., Tang, X.L., Yu, L.L., He, D., Zhao, S.: Calcined hydrotalcite-like compounds as catalysts for hydrolysis carbonyl sulfide at low temperature. Chem. Eng. J. **166**(1), 99–104 (2011)

Wang, L., Wang, S.D., Yuan, Q., Lu, G.Z.: COS hydrolysis in the presence of oxygen: Experiment and modeling. J. Nat. Gas Chem. **17**(1), 93–97 (2008)

Wang, X.Q., Ning, P., Shi, Y., Jiang, M.: Adsorption of low concentration phosphine in yellow phosphorus off-gas by impregnated activated carbon. J. Hazard. Mater. **171**(1–3), 588–593 (2009)

Wang, X.Q., Qiu, J., Ning, P., Ren, X.G., Li, Z.Y., Yin, Z.F., Chen, W., Liu, W.: Adsorption/desorption of low concentration of carbonyl sulfide by impregnated activated carbon under micro-oxygen conditions. J. Hazard. Mater. **229–230**, 128–136 (2012)

West, J., Williams, B.P., Young. N., Rhodes. C., Hutchings, G.J.: Ni- and Zn-promotion of γ-Al_2O_3 for the hydrolysis of COS under mild conditions. Catal. Commun. 2(3–4), 135–138 (2001)

Williams, B.P., Young, N.C., West, J., Rhodes, C., Hutchings, G.J.: Carbonyl sulphide hydrolysis using alumina catalysts. Catal. Today. **49**(1–3), 99–104 (1999)

Xiao, Y.H., Wang, S.D., Wu, D.Y., Yuan, Q.: Catalytic oxidation of hydrogen sulfide over unmodified and impregnated activated carbon. Sep. Purif. Technol. **59**(3,1), 326–332 (2008)

Yi, H.H., Yu, Q.F., Tang, X.L., Ning, P., Yang, L.P., Ye, Z.Q., Song, J.H.: Phosphine adsorption removal from yellow phosphorus tail gas over CuO–ZnO–La_2O_3/activated carbon. Ind. Eng. Chem. Res. **50**(7), 3960–3965 (2011)

Yu, M.X., Li, Z., Xia, Q.B., Xi, H.X., Wang, S.W.: Desorption activation energy of dibenzothiophene on the activated carbons modified by different metal salt solutions. Chem. Eng. J. **132**(1–3), 233–239 (2007)

Zhang, Y.Q., Xiao, Z.B., Ma, J.X.: Hydrolysis of carbonyl sulfide over rare earth oxysulfides. Appl. Catal. **48**(1,8), 57–63 (2004)

Zhao, S.Z., Yi, H.H., Tang, X.L., Ning, P., Wang, H.Y., He, D.: Effect of Ce-doping on catalysts derived from hydrotalcite-like precursors for COS hydrolysis. J. Rare Earths **28**(1), 329–333 (2010)